

## Domain observation and magnetostriction in Tb<sub>0.3</sub>Dy<sub>0.7</sub>Fe<sub>2</sub> twinned single crystals

J. P. Teter, K. Mahoney, M. Al-Jiboory, D. G. Lord, and O. D. McMasters

Citation: *Journal of Applied Physics* **69**, 5768 (1991); doi: 10.1063/1.348938

View online: <http://dx.doi.org/10.1063/1.348938>

View Table of Contents: <http://scitation.aip.org/content/aip/journal/jap/69/8?ver=pdfcov>

Published by the [AIP Publishing](#)

---

### Articles you may be interested in

[Microstructure and magnetostriction of \(Dy<sub>0.7</sub>Tb<sub>0.3</sub>\)<sub>1-x</sub>Pr<sub>x</sub>Fe<sub>1.85</sub> and \(Dy<sub>0.7</sub>Tb<sub>0.3</sub>\)<sub>0.7</sub>Pr<sub>0.3</sub>Fe<sub>y</sub> alloys](#)  
*Appl. Phys. Lett.* **69**, 3429 (1996); 10.1063/1.117282

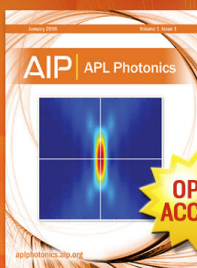
[Mn substitution effect on magnetostriction temperature dependence in Tb<sub>0.3</sub>Dy<sub>0.7</sub>Fe<sub>2</sub>](#)  
*Appl. Phys. Lett.* **61**, 114 (1992); 10.1063/1.107657

[A 3D anisotropic rotation model for magnetization and magnetostriction in Tb<sub>0.3</sub>Dy<sub>0.7</sub>Fe<sub>1.9</sub> \(abstract\)](#)  
*J. Appl. Phys.* **69**, 5797 (1991); 10.1063/1.347880

[Magnetostriction “jumps” in twinned Tb<sub>0.3</sub>Dy<sub>0.7</sub>Fe<sub>1.9</sub>](#)  
*J. Appl. Phys.* **63**, 3910 (1988); 10.1063/1.340602

[Liquid phase sintering of rare earth-iron \(Dy<sub>0.7</sub>Tb<sub>0.3</sub>Fe<sub>2</sub>\) magnetostrictive materials](#)  
*J. Appl. Phys.* **49**, 1972 (1978); 10.1063/1.324767

---



Launching in 2016!  
The future of applied photonics research is here



**AIP** | APL  
Photonics

## Domain observation and magnetostriction in $\text{Tb}_{0.3}\text{Dy}_{0.7}\text{Fe}_2$ twinned single crystals

J. P. Teter and K. Mahoney

*Naval Surface Warfare Center, 10901 New Hampshire Avenue, Silver Spring, Maryland 20903-5000*

M. Al-Jiboory and D. G. Lord

*Department of Pure and Applied Physics, University of Salford, Salford M5-4WT, United Kingdom*

O. D. McMasters

*Edge Technologies, Ames, Iowa 50011*

The ternary alloy  $\text{Tb}_{0.3}\text{Dy}_{0.7}\text{Fe}_2$  (Terfenol-D) exhibits the largest known magnetostriction to anisotropy ratio near room temperature. To better determine the interaction between the elastic and magnetic properties of this material, a stoichiometric twinned single crystal was grown by a free-standing float-zone technique. Observations using Scanning electron microscopy and energy dispersive spectroscopy confirmed that the sample was free of the normally present rare-earth (RE) eutectic phase and simultaneously free of Widmanstätten precipitate ( $\text{RE Fe}_3$ ). A bar with  $(111)$  and  $(1\bar{1}0)$  faces perpendicular to the  $[11\bar{2}]$  growth direction was examined. Also, a  $[11\bar{1}]$  slab was cut from the boule. This slab was studied along the  $[11\bar{1}]$  and  $[1\bar{1}0]$  directions with prestress applied along the  $[11\bar{1}]$ . This is the first report of the effects of applying prestress and magnetic fields in a direction not collinear with the  $[11\bar{2}]$  growth direction. From magnetization ( $M$ ) and magnetostriction ( $\lambda$ ) measurements as a function of field, prestress, and temperature, we determined the hysteresis and saturation parameters. These measurements do not indicate the  $[1\bar{1}0]$   $\lambda$  and  $M$  behaviors found previously for RE-rich Terfenol-D. Domain observations with differential phase contrast and x-ray topography have shown different orientations in the twin and parent sections of the  $[11\bar{1}]$  specimen. The observed structures can be interpreted as arising from domains with magnetization components normal to the surface. The domain observations on the  $(111)$  and  $(1\bar{1}0)$  bar faces and on the  $[11\bar{1}]$  slab correlate with each other with respect to orientations and domain interpretations.

### INTRODUCTION

The cubic Laves phase compound  $\text{Tb}_{0.3}\text{Dy}_{0.7}\text{Fe}_2$ , commercially known as Terfenol-D, exhibits a huge linear magnetostriction ( $\lambda$ ) with compensated magnetocrystalline energy near room temperature. Small single crystals have indicated that the magnetostriction arises solely from a large  $\lambda_{111}$  and that  $\lambda_{100} \ll \lambda_{111}$ . This large anisotropy in the cubic magnetostriction constants leads to a complex interaction between  $\lambda$  and the magnetization. In particular, the magnetization direction for maximum strain is not collinear with the strain measurement direction.<sup>1</sup> Large single crystals cannot presently be grown; however, bulk material can be grown in twinned dendritic sheets with the  $[11\bar{2}]$  axis as the growth direction.<sup>2</sup> This leads to an added complication in that the preferred  $\{111\}$  axes are not continuous across the twin or dendrite boundaries. Discontinuous changes in  $\lambda$  occur as the external magnetic field is increased in this material due to the magnetization vector jumping from the  $[111]$  axis to the  $[11\bar{1}]$  at  $19.5^\circ$  away from the  $[11\bar{2}]$  in the parent crystal.<sup>3</sup> The magnetostriction along the  $[111]$  and  $[1\bar{1}0]$  axes has been studied when the applied prestress and magnetic field is along the  $[11\bar{2}]$ .<sup>4</sup> These perpendicular directions yield  $\lambda$  dependencies that can be partially explained with the parent/twin magnetization model.<sup>3</sup> All of the twinned samples studied to date have

been iron deficient in order to suppress the formation of the rare-earth (RE)  $\text{Fe}_3$  phase.

In order to gain a better understanding of the interaction of the magnetization and magnetostriction constants in twinned single-crystal  $\text{Tb}_{0.3}\text{Dy}_{0.7}\text{Fe}_2$ , several stoichiometric crystals were grown and characterized. The  $[111]$  and  $[11\bar{2}]$  axes were examined with the applied field and prestress along the  $[11\bar{2}]$ . Also examined were the  $[11\bar{1}]$  and  $[1\bar{1}0]$  with prestress and magnetic field applied along the  $[11\bar{1}]$  direction. Figure 1 shows the relationship of these axes to each other. The magnetostriction and magnetization were studied as functions of compressive prestress, temperature, and magnetic field. Also, a more detailed study of the magnetism of the surface was obtained using x-ray-diffraction topography. The Berg-Barret technique is very useful for giving information on surface defects, such as magnetic domain structures. The contrast of the magnetic domains in x-ray topography arises as a consequence of the large magnetostrictive deformation of the lattice. This surface deformation can also be observed using optical microscopy.<sup>5</sup>

### EXPERIMENT

The pseudobinary compound  $\text{Tb}_{0.3}\text{Dy}_{0.7}\text{Fe}_2$  was prepared by a free-standing float-zone technique with a zone rate of 38 cm/h. The samples were then strain annealed.

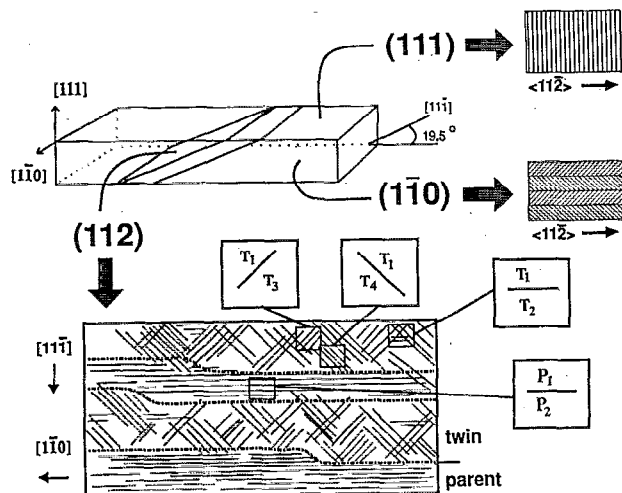


FIG. 1. Schematic drawing of the crystallographic orientation of the  $\text{Tb}_{0.3}\text{Dy}_{0.7}\text{Fe}_{1.98}$  bar and plate samples. The inset drawings are representative schematics of the magnetic domain patterns observed by DIC on the (112), (110), and (111) surfaces.

Initial characterization was accomplished by using oblique-incidence polarized light to detect the  $[11\bar{2}]$  dendritic platelet growth patterns. The samples were aligned by Laue x-ray diffraction and cut along the various crystallographic axes indicated in Fig. 1. Magnetization and magnetostriction properties were determined by a standard search coil with an integrating voltmeter and strain gauge techniques, respectively. The magnetization and magnetostriction were studied as functions of temperature from  $-60$  to  $90^\circ\text{C}$  using a Tenney environmental-control chamber and were studied as a function of applied compressive prestress using a support structure with a magnetically closed flux path.

The microstructure of the crystal surfaces was probed with a 20-keV scanning electron microscope (SEM) with 120-Å resolution which had an energy dispersive x-ray spectrometer (EDS) attachment for compositional studies. The magnetic and defect microstructure was examined using x-ray topographs taken at room temperature using a conventional x-ray generator with iron radiation, in the reflection (Bragg) geometry. A modified Berg-Barrett camera capable of stress and magnetic field applications was used. Zero-layer reflections of the  $[422]$  or  $[440]$  were obtained to ensure no image distortion.

The twin boundaries and domain structure can be observed using an optical microscope with polarized light and a Nomarski differential interference contrast (DIC) system. In conjunction with the DIC, observation of surface domains as a function of prestress and applied field was accomplished by use of a spring-tensioned specimen holder based around a C clamp which had modified pole faces and a 400-turn coil winding. This arrangement produced stresses up to 35 MPa and magnetic fields up to 500 Oe in a 1.5-cm gap.<sup>6</sup>

## DATA AND DISCUSSION

The SEM-EDS scans of each sample confirmed the absence of second phases and, in particular, the absence of

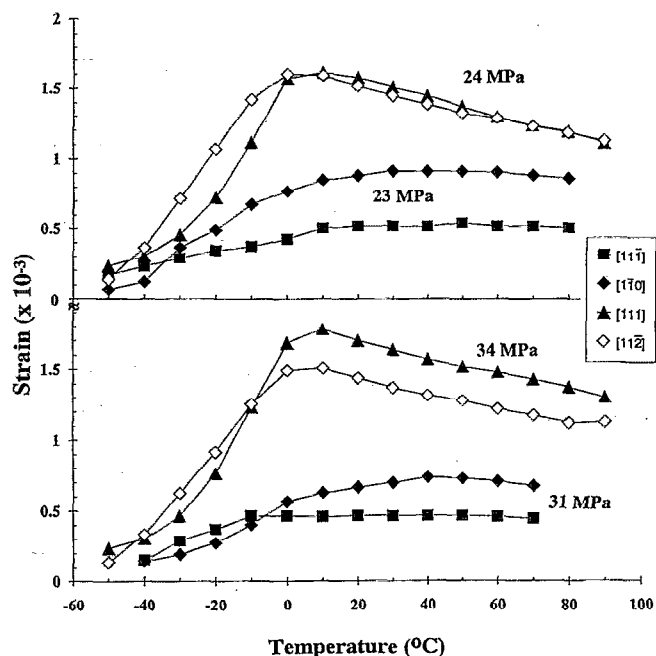


FIG. 2. Magnetostriction values at 1500 Oe for the  $[11\bar{2}]$ ,  $[111]$ ,  $[1\bar{1}0]$ , and  $[111]$  crystallographic directions vs temperature in Celsius. The upper curves were taken at  $\sim 24$  Mpa, while the bottom set of curves were taken at  $\sim 34$  MPa. Note that the applied magnetic field was colinear with the  $[11\bar{2}]$  for the  $[11\bar{2}]$  and  $[111]$  data sets, while the field was colinear with the  $[11\bar{1}]$  for the  $[11\bar{1}]$  and  $[1\bar{1}0]$  data sets. Also note that the  $[111]$  and  $[1\bar{1}0]$  curves exhibit negative magnetostriction in these cases.

Widmanstätten precipitate. The final stoichiometry of the samples was found to be  $\text{Tb}_{0.3}\text{Dy}_{0.7}\text{Fe}_{1.975}$ . A small region of one sample had a misaligned grain structure, and no data was taken from this region.

The magnetization versus field for the  $[11\bar{2}]$  field direction sample had the same functional form as reported previously.<sup>2</sup> The magnetization for the  $[11\bar{1}]$  field direction sample exhibited a 25% reduction in saturation moment relative to the  $[11\bar{2}]$  data, and less of the applied-field energy was being converted to magnetoelastic energy. In Fig. 2 the magnetostriction at 1500 Oe is shown as a function of temperature for two sets of applied compressive prestress. The  $\lambda$  data for prestress and field applied along the  $[11\bar{2}]$  growth direction clearly show the anisotropy compensation near room temperature and the large negative  $\lambda$  values for the  $[111]$  direction perpendicular to the  $[11\bar{2}]$ . The data for prestress and field applied along the  $[11\bar{1}]$  direction are not as easy to interpret, and here the position of the strain gauges is of critical importance for analysis. Note that here the  $[11\bar{1}]$  is positive, while the  $[1\bar{1}0]$  exhibits negative  $\lambda$ , i.e., contracts.

Shown in Fig. 3 are the strain variations with temperature observed in fields of 100 Oe. In such fields it is found that the magnetostriction changes sign to that found in higher fields (as shown previously in Fig. 2.).

The Berg-Barrett grazing incidence technique was used in the central region of the (112) plate where the strain gauges were attached. It was determined that the strain gauge measuring in the  $[11\bar{1}]$  direction was attached

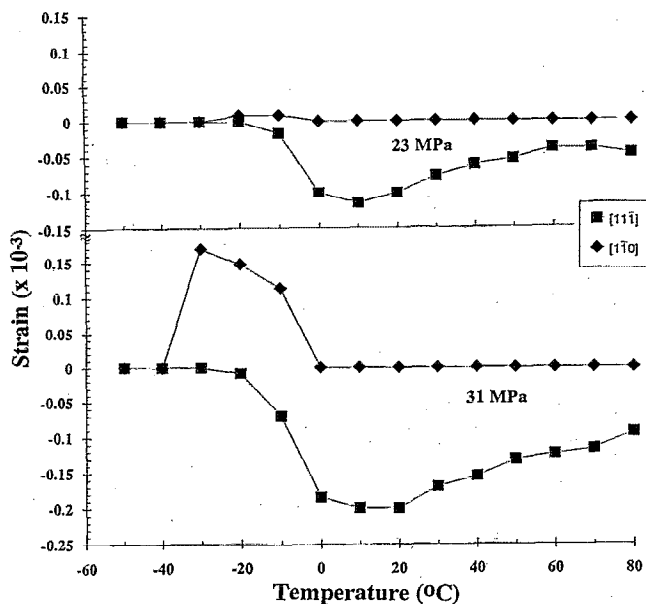


FIG. 3. Negative magnetostriction excursions at low magnetic field vs temperature for the  $[11\bar{1}]$ /twin and  $[1\bar{1}0]$  directions. The applied prestress and external magnetic field were colinear with the  $[111]$  direction. The value of the applied magnetic field where these minima occur is  $\pm 100$  Oe.

wholly on a twin section, while the  $[1\bar{1}0]$  gauge was on a parent section, separated by a twin boundary. The crystal was too strained for observation of the surface domain patterns. The domain structure is well defined, however, through the use of the optical DIC technique. Figure 4 shows an optical picture of the magnetic domains interacting through the magnetoelastic tensor to produce distortions on the crystal surface of the order of 10 nm.<sup>5</sup> This picture is schematically represented as the  $(1\bar{1}0)$  inset in Fig. 1.

The picture of the  $(1\bar{1}0)$  surface was taken at zero prestress and applied field. The domain patterns can be explained as arising from lattice distortions in neighboring domains with magnetization in the  $[111]$  and  $[1\bar{1}\bar{1}]$  direc-

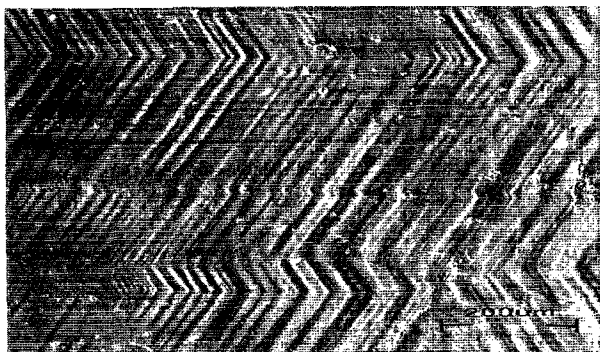


FIG. 4. Differential interference contrast picture of the  $(1\bar{1}0)$  plane showing the complex interplay of the moment vectors at the surface. Here, the major interaction is between the magnetization vectors across the  $[1\bar{1}\bar{1}]$  directions at  $70^\circ$  from the normal to the surface for both the parent and twin. There is a parent boundary running lengthwise across the photograph at each change of domain angle.

tions, causing a tilting in the  $(1\bar{1}0)$  surface plane for the parent. There is a similar symmetry for the twin. Both have the domain-wall plane normal to the  $[100]$  or  $[1\bar{0}0]$  and are  $109^\circ$  walls. The domain pattern for the  $(11\bar{1})$  plane is schematically shown in Fig. 1. Here, the distortion is caused by the  $\langle 111 \rangle$ 's that define the twin plane, labeled in the figure as  $P1/P2$ . The final bar surface, the  $(112)$  projection plane, is also shown in Fig. 1. Here, the symmetry between the twin and parent breaks down. For the parent, the domains and explanation are the same as for the  $(1\bar{1}0)$  surface. For the twin, the contrast comes from magnetization vectors arising from three competing symmetry planes. The schematic indicates  $T1/T3$  and  $T1/T4$  which are  $109^\circ$  and  $71^\circ$  walls normal to the  $[100]$  and  $[010]$ , respectively. The  $T1/T2$  distortions arise from  $109^\circ$  walls normal to  $[110]$ .

The DIC system was used along with an apparatus that applied a prestress and magnetic fields parallel to the  $[11\bar{2}]$ . The data were taken at room temperature and the  $(1\bar{1}0)$  surface was imaged. At high fields (500 Oe) and large applied compressive stresses (36 MPa), domain walls appeared that were perpendicular to the  $109^\circ$   $(100)$  walls. Also, at low fields (50–100 Oe) and small applied stresses (14 MPa), large-area subsurface domains modulated the surface at  $45^\circ$  to the applied field.

## SUMMARY

The magnetostriction and magnetization data presented for applied prestress and magnetic field along the  $[11\bar{2}]$  direction are well correlated with the optical topography work. A complete explanation of the effects of stress and field on this direction and on perpendicular directions is not presently known. The magnetostriction along the  $[11\bar{1}]$  exhibits the same dependencies with respect to applied prestress (there is a maximum  $\lambda$ ) and with respect to applied magnetic field as does the magnetostriction along the usual  $[11\bar{2}]$  growth direction. Therefore, the fit of the  $[11\bar{1}]$  and  $[1\bar{1}0]$  to the twin model is consistent with previous work.

This work was supported by the NAVSWC Independent Research Program Office.

<sup>1</sup>A. E. Clark, J. D. Verhoven, O. D. McMasters, and E. D. Gibson, IEEE Trans. Magn. MAG-22, 973 (1986).

<sup>2</sup>A. E. Clark, J. P. Teter, and O. D. McMasters, J. Appl. Phys. 63, 3910 (1988).

<sup>3</sup>J. P. Teter, A. E. Clark, and O. D. McMasters, J. Appl. Phys. 61, 3787 (1987).

<sup>4</sup>J. P. Teter, M. Wun-Fogle, A. E. Clark, and K. Mahoney, J. Appl. Phys. 67, 5004 (1990).

<sup>5</sup>D. G. Lord, V. Elliott, A. E. Clark, H. T. Savage, J. P. Teter, and O. D. McMasters, IEEE Trans. Magn. MAG-24, 1716 (1988).

<sup>6</sup>R. B. Coop, "Observations of Domain Structures in Terfenol-D under Stress," Physics Dept. internal report, University of Salford, 1989.